Short Communication

Development of Textured Al-doped Zinc oxide on the Glass Substrate with Pit Arrays for Thin Film Silicon Solar Cells

Hongyan Liu[1], Yushan Li[1], Hong Li[2,3]*

[1] Department of Physics, Heze University, Heze, 274015, PR China
[2] School of Physics and Electronic Information, Huaibei Normal University, Huaibei 235000, PR China
[3] Information College, Huaibei Normal University, Huaibei 235000, PR China
*E-mail: lihonggreat@126.com

Light trapping structure can increase the absorption of incident light. In this paper, we make used of porous anodic aluminum oxide as mask to fabricate the light trapping structure on the glass substrate before AZO film deposition. The average size of the pit is about 2 and 1μm, respectively. It was found that the efficiency of the n-i-p solar cells using AZO film with pit arrays as back surface reflectors have obvious improvement. Furthermore, we improved the external quantum efficiency of the solar cells in the infrared region.

1. INTRODUCTION

Transparent conducting oxides (TCOs) have attracted great interest in solar cells due to their higher optical transparency and lower electrical conductivity [1-3]. Out of the many TCOs, Al-doped zinc oxide (AZO) is the most frequently used material because its surface morphology is easy to be modified through many methods [4,5], such as sputtering, pulsed laser deposition, hydrothermal method, chemical vapor deposition and so on. Further, AZO is highly durable against hydrogen plasma. For solar cells, light trapping is very important to obtain a higher efficiency [6-10], because the appropriate light trapping structures can scatter the incident light and subsequently to improve the conversion efficiency.

It is suggested that light trapping can be realized through the textured surface. Usually, there were two methods to fabricate AZO film with textured surface. The first is etching the substrate first,

and then deposit the AZO film on the etched substrate. Hongsingthong [11] used the standard reactive ion etching process to etch the glass substrate before AZO film was deposited. The results showed that the properties of solar cells using the AZO film on the textured surface were improved compared to solar cells using the AZO film deposited on the flat glass substrate. The second is the AZO film was deposited on the substrate first and subsequent was etched. Wang [12] deposited the AZO film on the flat glass substrate and then used the Hydrochloric acid solution to make the AZO film with broad surface feature distributions. Experimental results suggested that the developed AZO film enhanced the short circuit current density and conversion efficiency without reduction in fill factor and open circuit voltage.

In this paper, The Al layer were deposited on the glass substrate, followed by anodization in phosphoric acid and critic acid solutions respectively under the different voltages to obtain porous anodic aluminum oxide with two different diameters on the glasses. Then the glasses with porous anodic aluminum oxide were subjected to wet chemical etching in hydrofluoric acid solution. So, we successfully get the glass substrate with light trapping structure. The efficiency of the n-i-p solar cells with the light trapping structure which was improved from 4.57 to 5.03% compared to flat glass substrate.

2. EXPERIMENTAL

2.1. substrate preparation

The corning 7059 glasses were sequentially cleaned with ethanol, acetone, and deionized water before being dried at 80 ℃ for 10 min. Al film with a thickness of 2 μm was grown on the glass substrates with the radio frequency sputtering and sputtering powder 200 W, respectively. Afterward, the substrate was anodized at 195 V for 60 s in 0.25 M phosphoric acid solution, the temperature of condensate tank was set to minus 4 ℃. Then the substrate was exposed to 0.5 wt% phosphoric acid solution at 45 ℃ for 45 min. Another substrate was anodized at 40 V for 30 min in 0.3 M oxalic acid solution at 4 ℃. Subsequently, it was activated by immersing in 0.5 wt% phosphoric acid solutions at 45 ℃ for about 20 min. and then the two substrates were etched with 40 wt% hydrofluoric acid solutions for 10 s. In the end, the two substrates were rinsed with deionized water and dried in the air.

2.2. Solar cell fabrication

n-i-p thin film silicon solar cells with an area of 1 cm^2 were produced on the etched glass substrate coated with Ag/AZO as back surface reflectors. The detailed structure of the solar cells was glass substrate Ag (100 nm)/AZO (30 nm)/μc-Si:H/n-i-p/In$_2$O$_3$:Sn (ITO, 75 nm)/Ag grid. For comparison, n-i-p thin film silicon solar cells were also produced on the flat glass with the same parameters.

2.3. characterization

Surface morphology of the etched substrate was evaluated by field emission scanning electron microscope (SEM). The reflectance of back surface reflectors was ultraviolet-visible light spectrometer in wavelength range 300-1100 nm. The current-voltage and characteristics of the solar cells were measured by AM 1.5 spectrum at room temperature.

3. RESULTS AND DISCUSSION

The schematic description of the entire experiment process is shown in Fig.1. First, a clean piece of corning 7059 glasses is used as the substrate. Second, Al film is deposited on the glass substrate, and the thickness of Al film is about 2 μm. Third, the porous anodic aluminum oxide is fabricated by anodization process. At last, using the porous anodic aluminum oxide as mask, the sample is etched by the 40% wt hydrofluoric acid solution for 10 s to obtain textured surface.

Fig. 2 displays the SEM images of porous anodic aluminum oxide which are fabricated on the glass substrate. Fig. 2(a) and (b) show the top surface image and cross section image of porous anodic aluminum oxide which was anodized in the phosphoric acid solution. The images show that the porous anodic aluminum oxide is highly ordered and the pore diameters range from 200 to 300 nm. Fig. 2(c) and (d) show the top surface image and cross image of porous anodic aluminum oxide which was
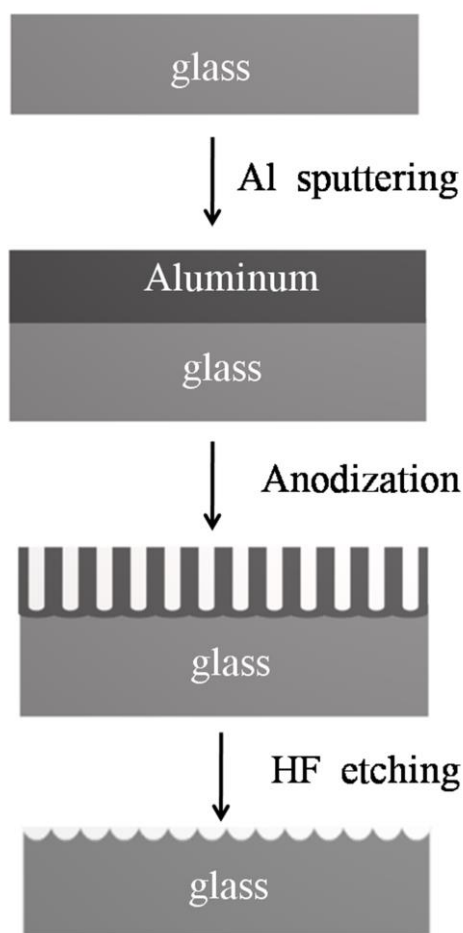

Figure 1. The schematic diagram of the entire experiment process.
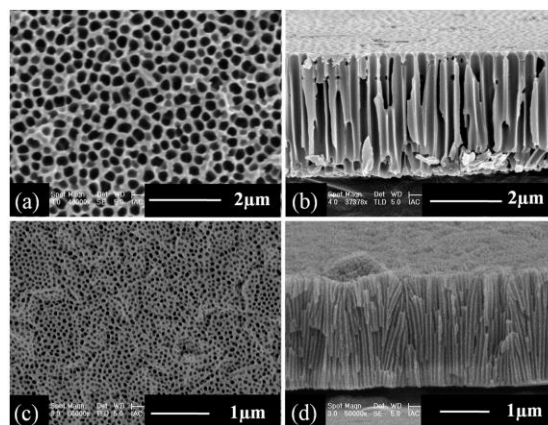
Figure 2. SEM images of porous anodic aluminum oxide which are fabricated on the glass substrate. (a) Top surface image and (b) cross section image of porous anodic aluminum oxide which were anodized in the phosphoric acid solution. (c) Top surface image and (d) cross image of porous anodic aluminum oxide which were anodized in the oxalic acid solution

anodized in the oxalic acid solution. And the pore diameters are in the range from 80 to150 nm. It is seen from Fig. 2(b) and (d) that these pores can reach the glass substrate directly. We can conclude that the pore diameters of porous anodic aluminum oxide can be easily regulated by anodization process with different oxidation electrolytes.
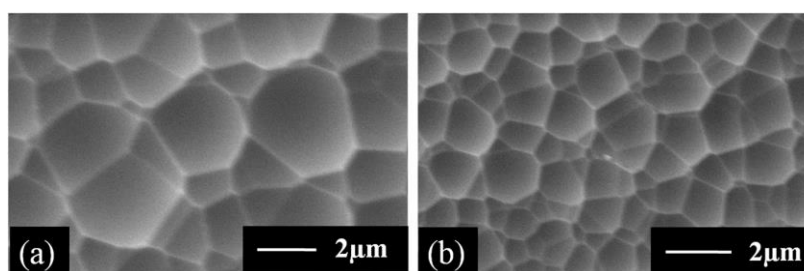

Figure 3. SEM images of the pit arrays obtained on the two substrates, respectively.

After wet etching by hydrofluoric acid solution, the surface of glass surface form pit arrays. Fig. 3(a) and Fig. 3(b) show the SEM images of the pit arrays obtained on the two substrates, respectively. It can be seen in Fig. 3(a) and Fig. 3(b) that average size of the pit is about $\Lambda = 2$ μm and $\Lambda = 1$μm, respectively. We can conclude that in the process of wet etching, the effect of porous anodic aluminum oxide is as a mask. The size of pit increases with the increasement of pore diameter of porous anodic aluminum oxide. This is the reason for the formation of pit arrays.

Fig. 4 depicts the total reflection spectra of three back reflectors, where the flat and $\Lambda = 1$ and 2 μm glass substrates coated by Ag (100 nm) using sputtering method. It can be seen in Fig. 4(a) that the total reflection spectrums of three back reflectors slightly reduce with the increase of average size of pit arrays, However, the range of decrease is small and more than 90% in the near infrared region.
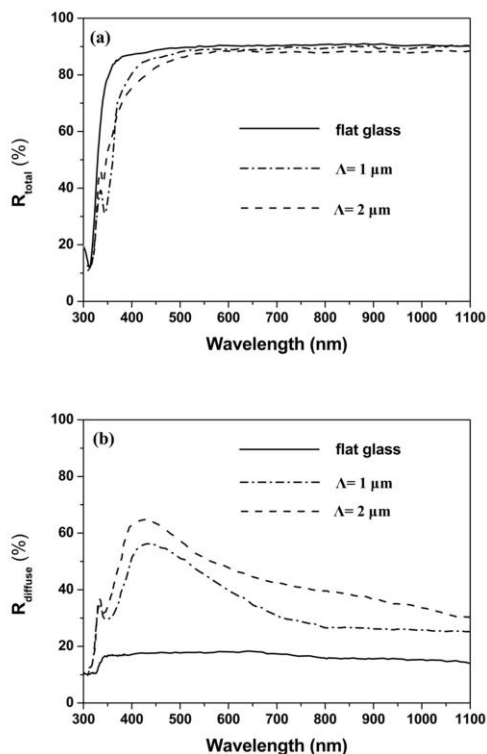
Figure 4. (a) Total reflectivity and (b) diffuse reflectivity spectra of the three back reflectors which were coated by Ag film.
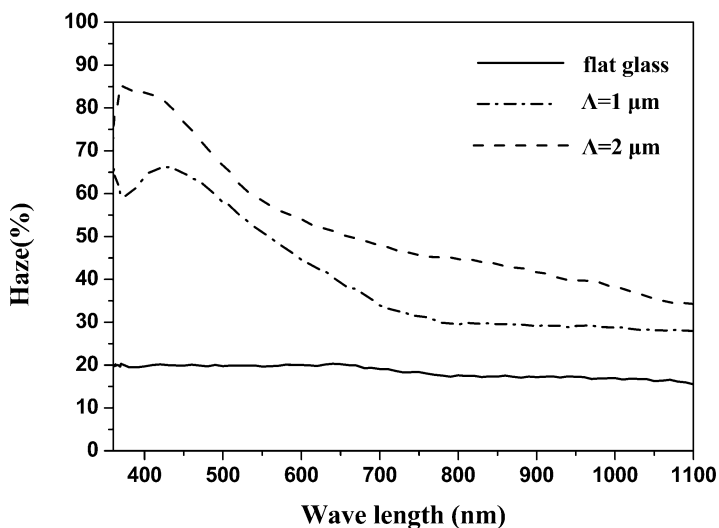
Figure 5. Haze spectra of the three back reflectors

In addition, the three back reflectors have absorption peak near the wavelength of 350 nm, and its intensity of the peaks is sharply increased with the increase of average size of pit arrays. The increase of absorption peak intensity with increasing size of pit arrays can be explained by localized surface plasmon resonance [13] of Ag nanostructures. There will be stronger localized surface plasmon resonance absorption with the degree of nanostructure.
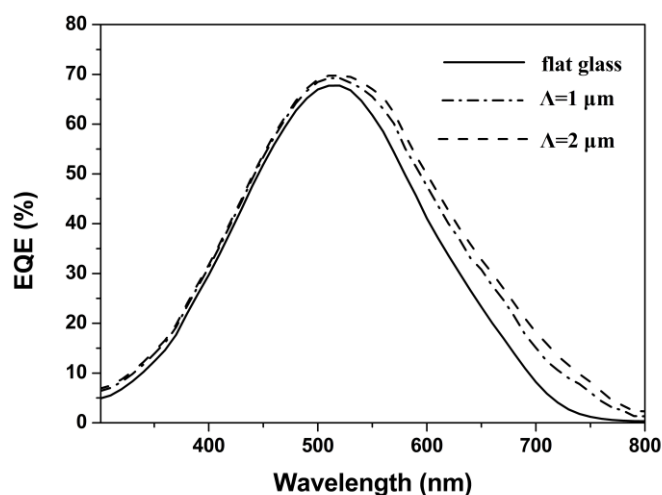
Figure 6. External quantum efficiency (EQE) spectra of three kind of n-i-p thin film silicon solar cells which were prepared on the flat, and patterned glass with Λ =1 and 2 μm

Fig. 4(b) illustrates the diffuse reflection of three back reflectors. As shown in Fig. 4(b), the intensity of diffuse reflection increases with the increasing average size of pit arrays. These show that pit arrays on the glass substrate have good light trapping properties. Haze ratio is one of the most important parameters of textured surface and can improves the light scattering in AZO Films [14,15]. The value of haze ratio is defined as

$$\text{Haze} = \frac{diffuse\ reflectivity}{\text{total}\ reflectivity} \times 100\%$$

Fig. 6 gives the haze spectra of the three back reflectors. The average value of haze of three back reflectors is about 18.44, 42.67 and 54.60% in the range from 350 to 1100 nm. In reference [14], The average value of haze is about 5.61, 19.21, and 22.07% respectively. So we can conclude that this textured surface can improve the short circuit efficiency, and eventually improve the conversion efficiency of solar cells.

The n-i-p thin film silicon solar cells were prepared on flat, and patterned glass with Λ =1 and 2 μm, respectively. Fig. 6 exhibits the external quantum efficiency (EQE) spectrum of three n-i-p thin film silicon solar cells. The solar cells on the patterned glass substrate have much higher EQE values than that of cell on flat glass in the wavelength range of higher than 550 nm. In addition, the EQE value has obvious improvement with the increase of Λ.This result can be verified by the increase of diffuse reflectivity with the increase of Λ in the wavelength range more than 550 nm. Table 1 shows the open-circuit voltage (V_{oc}), short-circuit current (J_{sc}), fill factor (FF), and efficiency of the n-i-p thin film silicon solar cells. It can be seen in Table 1 that FF has a little decrease as often observed in thin film silicon solar cells. However, the V_{oc}, and J_{sc}, have obvious improvement with the increase of Λ.Compared with n-i-p thin film silicon solar cells developed on the flat glass, the efficiency of n-i-p thin film silicon solar cells developed on the patterned structure increased by 10%. This result indicates

that the pit arrays formed on the glass has a good light trapping effect. Many parameters are not optimized in the fabrication of thin silicon solar cells, so the efficiency is lower compared to the results reported in the literature reference [14,15] recently.

Table 1. Characteristics of n-i-p thin film silicon solar cells which were prepared on the flat, and patterned glass with $\Lambda = 1$ and 2 μm.

Sample	V_{oc} (V)	FF (%)	Eff (%)	J_{sc} (mA/cm^2)
flat glass	0.787	58.7	4.57	9.91
Λ=1 μm	0.812	58.1	4.89	10.1
Λ=2 μm	0.838	56.8	5.03	10.6

4. CONCLUSIONS

In order to enhance the performances of n-i-p thin film silicon solar cells, the porous anodic aluminum oxide with the function of mask has been prepared by Anodic oxidation method. On this basis back surface reflectors with light trapping structure were developed by etching method. By this method, the performances of the n-i-p thin film silicon solar cells have obvious increase. We expect that the efficiencies of n-i-p thin film silicon solar cells can be improved by optimizing the size and shape of pit arrays on back surface reflectors.

References

1. J. Buckeridge, C.R.A. Catlow, M.R. farrow, A.J. Logsdail, D.O. Scanlon, T.W. Keal, P. Sherwood, S.M. Woodley, A.A. Sokol, A. Walsh, *Phys. Rev. Mater.,* 2 (2018) 323.
2. K. Yoon, C. Shin, Y. J. Lee, Y. Kim, H. Park, S. Baek, J. Yi, *Mater. Res. Bull.,* 47 (2012) 3023.
3. I. Saadeddin, H. S. Hilal, R, Decourt, G. Campet, B. Pecquenard, *Solid State Sci.,* 14 (2012) 914.
4. S. Bose, R. Arokiyadoss, P.B. Bhargav, G. Ahmad, S. Mandal, A.K. Barua, S. Mukhopadhyay, *Mat. Sci. Semicon. Proc.,* 79 (2018) 135.
5. S.Q. Hussain, A.H.T. Le, K. Mallem, H. Park, M. Ju, Y. Kim, J. Cho, J. Park, Y. Kim, J. Yi, *Appl. Surf. Sci.*, 447 (2018) 866.
6. Z. Ghorannevis, E. Akbarnejad, A.S. Elahi, M. Ghoranneviss, J. Cryst. Growth, 490 (2018) 117.
7. Y. Wang, W.W. Jiang, W.Y. Ding, W.P. Chai, J. Mater. Sci-Mater. El., 28 (2018) 3530.
8. W.M. Li, H.Y. Hao, M. He, J. Xing, H. Gao, J.J. Dong, *Surf. Coat. Tech.,* 258 (2014) 991.
9. Y.F. Wang, J.M. Song, G.Z. Niu, Z.H. Yang, Z.W. Wang, X.D. Meng, F. Yang, J.Y. Nan, *Cream. Int.,* 43 (2017) 9382.
10. S. Bos, A. Rayarfrancis, P.B. Bhargav, G. Ahmad, S. Mukhopadhyays, S. Mandal, A.K. Barua, *J.*

     Mater. Sci-Mater. El., 29 (2018) 3210.
11. A. Hongsingthong, T. Krajangsang, A. Limmanee, K. Sriprapha, J. Sritharathikhun, M, Konagai, *Thin Solid Films,* 537 (2013) 291.
12. Y. F. Wang, X. D. Zhang, L. S. Bai, Q. Huang, C. C. Wei, Y. Zhao, *Appl. Phys. Lett.,* 100 (2012) 263508.
13. H. Sai, M. Kondo, *J. Appl. Phys*., 105 (2009) 094511.
14. G. Das, S. Bose, J.R. Sharm, S. Mukhopahyay, A.K. Barua, *J. Mater. Sci-Mater. El.,* 29 (2018) 6206.
15. S.Q. Hussain, A.H.T. Le, K. Mallem, H. Park, M. Ju, Y. Kim, J. Cho, J. Park, Y. kim, J. Yi, Appl. Surf. Sci., 447 (2018) 866.